
SPARSE MULTIMODAL FUSION WITH MODAL CHANNEL ATTENTION

A PREPRINT

Josiah Bjorgaard¹

¹*Syntensor, Inc.*

1 Abstract

The ability of masked multimodal transformer architectures to learn a robust embedding space when modality samples are sparsely aligned is studied by measuring the quality of generated embedding spaces as a function of modal sparsity. An extension to the masked multimodal transformer model is proposed which incorporates modal-incomplete channels in the multihead attention mechanism called modal channel attention (MCA). Two datasets with 4 modalities are used, CMU-MOSEI for multimodal sentiment recognition and TCGA for multiomics. Models are shown to learn uniform and aligned embedding spaces with only two out of four modalities in most samples. It was found that, even with no modal sparsity, the proposed MCA mechanism improves the quality of generated embedding spaces, recall metrics, and subsequent performance on downstream tasks.

2 Introduction

Multimodal models are increasingly becoming the norm for deep learning applications. [1–3] Many studies use model trained with two aligned modalities. [4–10, 10–13], including incorporating images into large language models. [14, 15] Training models with more than two aligned modalities has also been studied, [6, 16–21], and recent examples explore learning from multiple unaligned or partially aligned modalities [22–27].

Most of these examples use a combination of text, audio, image and video. However, applications can use data other than these traditional media formats. For example, multisensor fusion in home monitoring systems and robotics includes tabular sensor data and time series data from different types of sensors. [28]. Bioinformatics and biomedical applications use data that consists of tabular, image, and sequence data. In these fields, each media format in the data can also be comprised of different modalities having the same data type but different data source, for example as in two tables of data from different types of experiments. [29]

Contrastive learning of multimodal data is an important class of multimodal model. [5–8, 17, 30] In the well-known CLIP model, it generates joint embeddings for modalities, which can be used for multi-modal classification and regression or for conditioning of diffusion probabilistic models. These embeddings can also be used for multi-modal retrieval, such as in Everthing At Once where video retrieval can be performed via text or audio via a trimodal embedding. As the number of modalities used for training a model increases, modal-incomplete samples are more likely to occur. Modal fusion models which can not include modal-incomplete samples are thus not well suited to be used for applications with datasets that have many modalities.

There are a few approaches which can achieve self-supervised learning with modal-incomplete samples outside of contrastive representation learning. Interleaved data can use incomplete modalities due to their treatment of samples as a sequence. [14] Similarly, masking of the model in a late stage fusion block can be used [21, 25]. These model architectures require an autoregressive or a masked language objective in order to train on the interleaved data or predict missing data. These types of models may be incompatible with objectives where an embedding at inference time should be equivalent whether or not a modality is missing from the sample being embedded. For example, given a sample with 3 modalities, it would not be possible to generate embeddings from any combination of only 2 of the modalities which are all numerically similar.

Recent studies have shown that using contrastive learning between unimodal representations and a learnable fusion representation can generate useful joint embeddings. [18, 20] This type of model uses block attention masking to effectively perform self-attention on unimodal representations and cross-attention with a fused representation in the attention block. However, the application of this masked multimodal attention (MMA) model architecture to datasets which are modality incomplete is yet underexplored. This study aims to show that masked multimodal attention functions well even when modalities are sparsely aligned. We propose an extension of the masked multimodal transformer model that incorporates modal-incomplete channels in the multihead attention block called modal channel attention (MCA). Using two well-known datasets, each with four modalities, both models are shown to learn quality embedding spaces up to a sparsity level of at least 40%, corresponding to an average number of modalities per sample of 2.4. We find that MCA generally improves the quality of generated embedding spaces, recall metrics, and subsequent performance on downstream tasks by linear probing. We conclude with a discussion on potential applications and directions for future work.

3 Related Work

The Everything At Once [17] model uses a transformer encoding of multiple modalities (i.e. a fusion transformer) with contrastive loss. The fusion transformer is applied multiple times per minibatch in order to formulate embeddings for each modality and each pair of modalities. These embeddings are applied in a combinatorial contrastive loss function. The final unimodal and bimodal embeddings are pooled and projected to a multimodal embedding space. This method requires a number of forward passes that scales exponentially with the number of modalities, which is undesirable for computational efficiency and scalability.

FLAVA [7] uses multiple loss models for data which is missing a modalities. For example, with language they use a masked language objective, while for image-text pairs, they use a contrastive loss. Their approach allows for unimodal and multimodal inference, but does not generate a multimodal fusion embedding space. Similarly, Zhang et al. developed a model which can be trained with missing modality combinations. [23] The model projects unimodal encodings into a modality-aligned feature space, and then performs weight-shared dual attention prediction of two sets of outputs. The first output is trained with supervision to class labels, while the second prediction is trained with supervision to unimodal predictions across epochs. This is shown to improve predictions for unseen modalities.

Another approach by Wei et al. uses a multimodal fusion model that is trained to generate missing modalities. [26] A similar approach was taken with LORRETA using an objective of predicting a third modality given two other modalities. This approach requires bimodal pairs for each forward pass and can not directly embed higher order modality combinations. [25] Neither approach generates a fused embedding space that is directly applicable to tasks based on the fused data embeddings such as retrieval or linear probing.

Zorro is an MMA model which produces both unimodal and multimodal outputs trained with a contrastive loss. [18] A similar MMA architecture was recently applied by Shi et al. in order to fuse 3 modalities for image segmentation in a biomedical application. [20] While the latter study notes that MMA seemed to function well with missing modalities, they did not directly explore the performance of this type of modal fusion with sparsely aligned multimodal data.

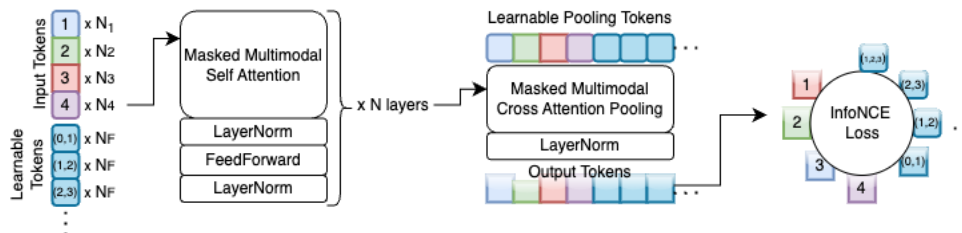


Figure 1: Overall model architecture demonstrating a single forward pass. N_i represents the number of tokens. The model architecture is related to models present in Refs. [17] and [18].

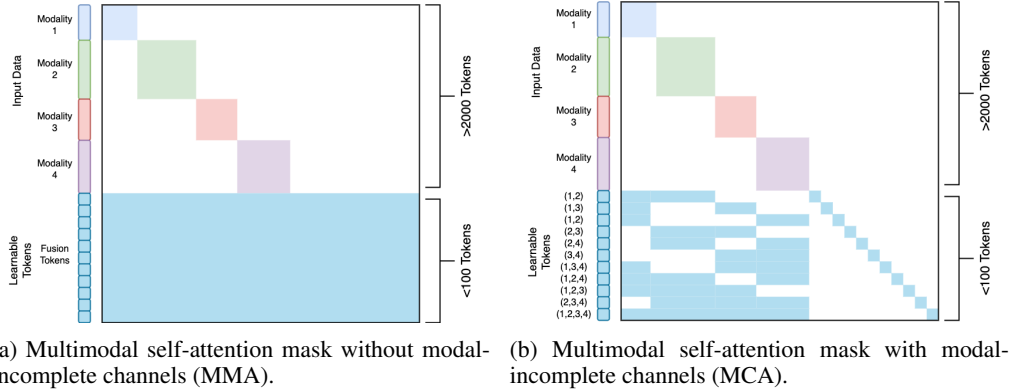


Figure 2: Comparison of self attention masks used in this study. The attention mask on the left is based on the attention mask used in Ref. [18] and the mask on the right is the proposed MCA mask. Token numbers are condensed for space and are not proportional to the quantity of tokens used.

4 Model

The studied model architecture is presented in Figure 1. It consists of a transformer encoder with learnable pooling layer and noise contrastive estimation (NCE) loss between pooled tokens. Also used in this study are trainable transformations on the input data - linear transformations or MLPs which are applied on a token-by-token basis in order to encode tabular data or compress pretrained frozen embeddings as inputs. The attention model uses MMA. MMA uses fusion token blocks which are attended by unimodal token blocks. Unimodal token blocks are only able to self-attend, as shown in Figure 2a.

This study introduces multi-channel attention into MMA, where blocks of fusion attention are only attended to by a subset of the modalities. In contrast to the method of Ref [17], this maintains the efficiency of using a single forward pass per sample, regardless of the number of modalities present in the sample. Each fusion channel corresponds to the fusion of a different set of modalities as shown in Figure 2b. In the learnable pooling layer, each fusion channel corresponds to a unique pooling token. NCE Loss is applied between each pair of unimodal and fusion channel tokens. The fusion channel which is attended to by all modalities is taken as the fusion embedding for embedding space analyses and downstream tasks. The learnable pooling layer has a similar multimodal mask, preventing fusion tokens from attending to unimodal tokens. The pooled layer includes a token for each modality and each type of fusion.

For this study, 5 transformer encoder layers are used, each with a hidden size of 512 and 8 attention heads. The feed-forward layers use a feed-forward multiplier of 4 and the GeGLU activation function. There are a total of 88 fusion tokens in both studied models. In the masked multimodal transformer, all 88 fusion tokens are pooled in the pooling layer, while in the MCA transformer, each channel uses 8 tokens and 11 channels are present as shown in Figure 2b. As described above, each set of 8 tokens is pooled separately in the pooling layer. Importantly, there are an identical number of trainable input tokens in each model and a nearly equal number of parameters, increased in MCA only by 10 additional learnable pooling tokens in the pooling layer.

5 Methods

5.1 Datasets

5.1.1 CMU-MOSEI

The CMU-MOSEI was obtained and processed using the mmdatask Version 1.1 using the included word level alignment example. This results in 23248 samples of aligned unimodally embedded data corresponding to glove vector, OpenFace, COVAREP, and FACET encoders. [31] A test split is randomly chosen with 2324 samples.

For each modality, a sample is a series of embeddings for multiple time steps. The number of vectors vary per sample, due to the embedded video clips having varying duration. To prepare the modalities for input into the transformer block, each vector in a sample is transformed by using a linear layer and layer normalization, resulting in a token embedding size of N_{emb} . This normalized, transformed vector is then added to a standard sinusoidal positional

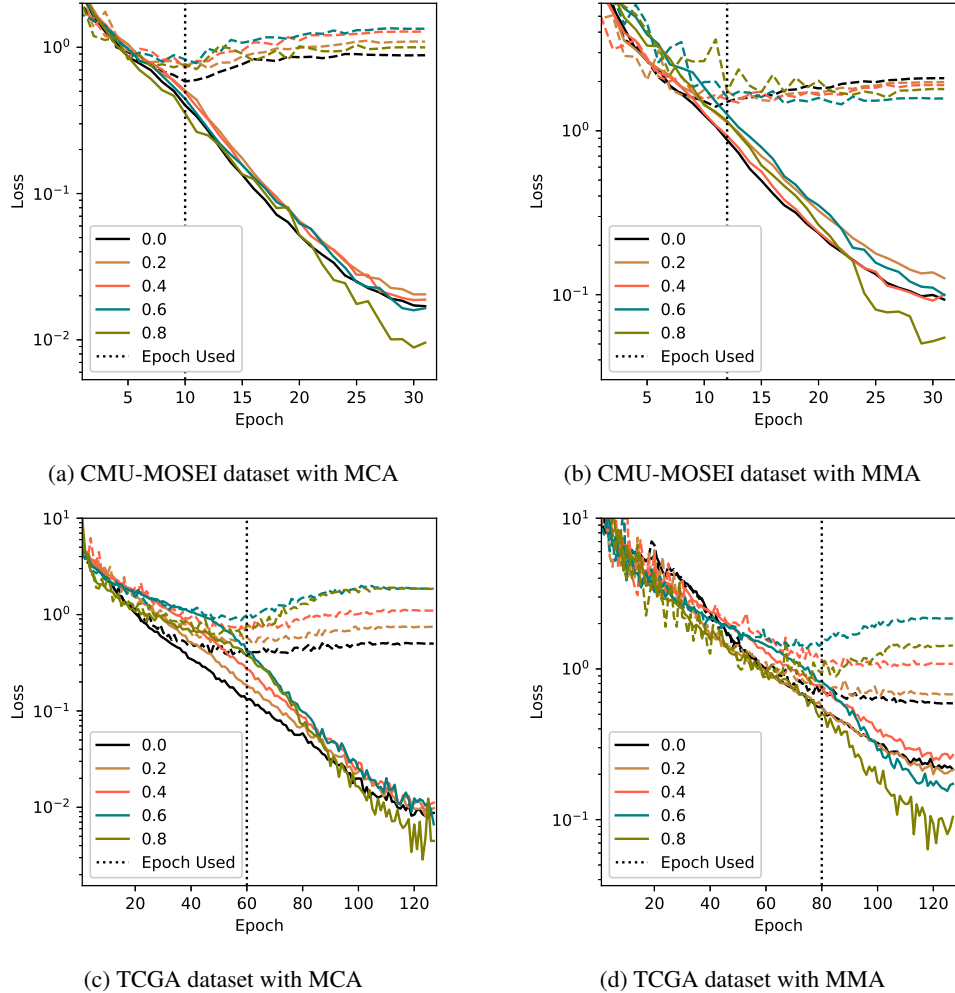


Figure 3: Epoch averaged losses at various modal sparsities (legend) for train (solid lines) and test (dashed lines) splits, trained with either the MCA or MMA models on either CMU-MOSEI or TCGA datasets.

embedding vector to encode it’s position in the sequence of vectors for a given modality. No other learnable token embedding is used for these samples. The result of this process is that each sample token is transformed into a token for input in to model studied in this paper

5.1.2 TCGA

The Cancer Genome Atlas (TCGA) [32] provides a multi-omics dataset that consisting of tabular data for gene expression, reverse phase protein arrays (RPPA), DNA methylation, and miRNA measurements. This data was downloaded from the supporting information of Ref [32]. To reduce the number of gene expression and DNA methylation columns in the dataset, the top 800 genes and methylation sites with the highest variance were used to create a signature of the gene expression and methylation data. For RPPA data and miRNA tables, there are 198 protein columns and 662 MiRNA columns. To align unimodal samples into a multimodal dataset, we use provided identification numbers for patient and sample, resulting in an intersection of 7017 samples that have all modalities. A test split is randomly chosen with 707 samples.

To prepare TCGA tables for the MCA and MMA encoders, tabular values are passed tokenwise through a trainable 2 layer MLP($1, N_{emb}, N_{emb}$) and ReLU activation function. This allows a continuous representation of the tabular value into a vector with the same size as the transformer encoder embedding space N_{emb} . The tabular column index is encoded with the standard learnable embedding vector of size N_{emb} for each index. The value and column index encodings are added together to form the initial embedding vectors for the transformer encoders.

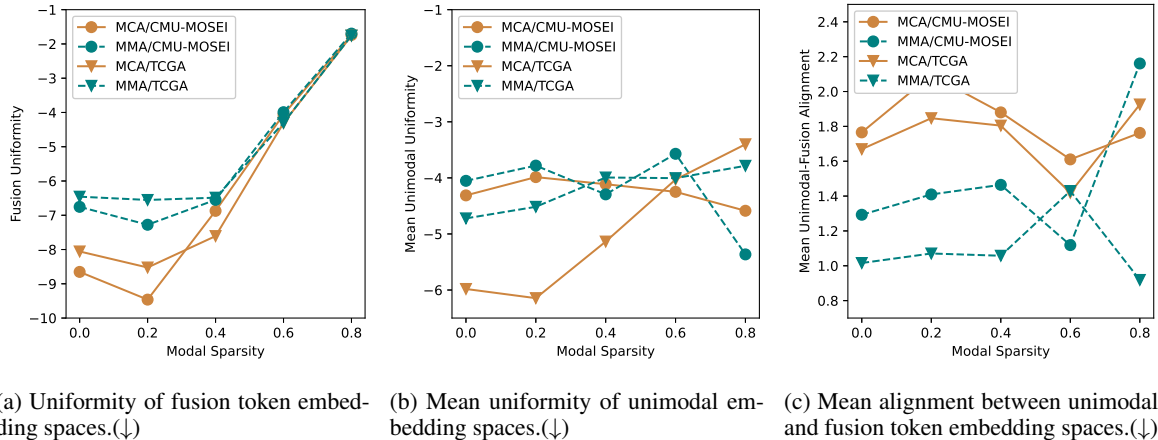


Figure 4: Uniformity and alignment metrics as a function of dataset sparsity for CMU-MOSEI and TCGA dataset embeddings calculated from the test dataset splits.

5.2 Modal Sparsity

In order to evaluate the performance of masked multimodal attention with missing modalities, unimodal samples are dropped from the datasets. Randomly selected samples are dropped uniquely for each modality with a probability defined herein as the modal sparsity. The modal sparsity reported in the following figures represents the fraction of dropped samples in each modality. Due to the training cost of many models, experiments were performed with datasets corresponding to 0, 0.2, 0.4, 0.6, and 0.8 modal sparsity.

Since both datasets used in this study contain 4 modalities, a modal sparsity of 0.2 indicates that most samples have 3 modalities present, while at a modal sparsity of 0.6 indicates that most samples have only 1 or 2 modalities present. When a modality is dropped from a sample, a padding token is used for all tokens corresponding to that modality such that they are masked from subsequent attention blocks and subsequent loss function terms are dropped. When all modalities attending to a specific fusion channel are masked, InfoNCE loss function terms using the corresponding token are also eliminated from the loss function.

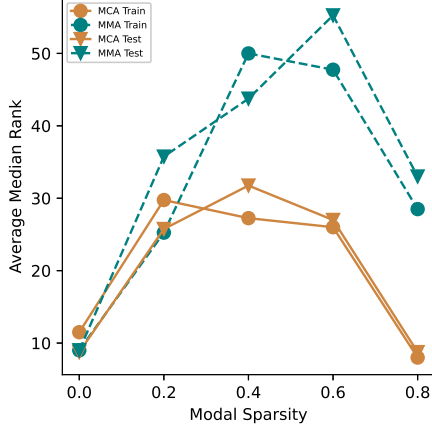
5.3 Training

Training was performed for each model on 4xA10G Nvidia GPUs. Hyperparameters were chosen identically for MMA and MCA experiments. An effective batch size of 32 and cosine scheduled learning rate with a maximum of 10^{-4} and warm up of 2000 steps is used for all experiments. Test splits of datasets were selected randomly as a fraction of 0.15 of a dataset. For CMU-MOSEI experiments, 32 epochs are trained. For TCGA fusion, 128 epochs are trained. The epoch number selected for evaluating embeddings was hand selected by identifying the best set of eval loss scores for a model/dataset pair at all modal sparsities as shown in Fig. 3. The model and training code were developed using the Pytorch 2.1. [33]

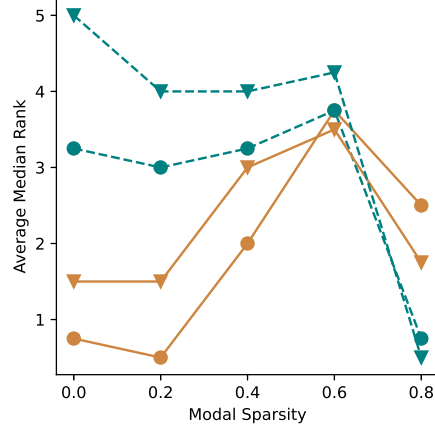
6 Evaluation of Embeddings

This section aims to analyze the characteristics of the embeddings produced by the trained models. Embedding spaces trained with contrastive learning are characterized by alignment and uniformity. [24] Alignment and uniformity were calculated according to Ref. [24] with the test split of the datasets. The results of averaging these quantities over the unimodal embeddings produced by a given model are displayed in Figure 4, while additional plots for each modality are included in Section 9.

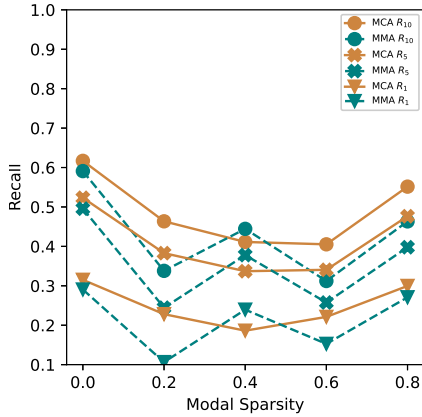
If a model is trained to generate an embedding space with lower uniformity (indicating a more uniform embedding space), the alignment of positive examples will tend to be decreased. [24] The uniformity of MCA is significantly lower (improved), producing a more uniform embedding space than MMA, while the alignment is increased (worsened). The alignment is calculated here for the complete (all modality) fusion channel in MCA, while the loss in MCA calculated with multiple fusion channels. As the modal sparsity is increased beyond 40%, both model’s fusion uniformities increased (worsened). The unimodal uniformity also increased, indicating less uniform unimodal embedding spaces. The alignment, however, does not change significantly as the modal sparsity is increased.



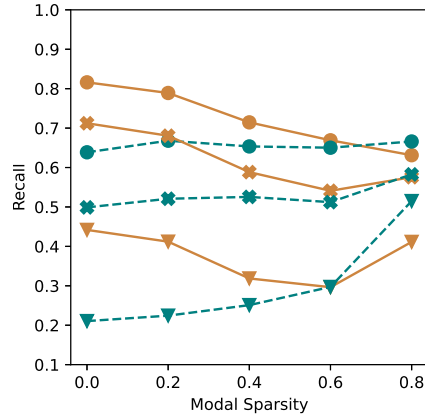
(a) Modal average of Median Rank for CMU-MOSEI (↓)



(b) Modal average of Median Rank for TCGA (↓)



(c) Modal average of Recall for CMU-MOSEI (↑)



(d) Modal average Recall for TCGA (↑)

Figure 5: Recall metrics for embeddings from models trained with various modal sparsity on the CMU-MOSEI and TCGA datasets. Recall metrics are calculated for recall from test dataset split embeddings to all dataset embeddings (train and test splits),

Recall metrics were examined for the generated validation datasets (median rank, R_1 , R_5 , and R_{10}). These recall metrics demonstrate the ability of the model to use a unimodal embedding to recall a fused embedding. Both MMA and MCA architectures always produce the same unimodal embeddings for a given set of unimodal tokens, regardless of whether other modalities are absent, or different from multimodal samples on which the model is trained. Here, the rank is defined as the median of the ranks of a matched fusion embedding vector to a unimodal embeddings in the ranked set of cosine similarities between a single unimodal embeddings and each fusion embedding.

The median rank is the median of these ranks for all unimodal embeddings. The R_x metric is the probability that the correct embedding vector is in the top x most similar fusion embeddings to a unimodal embedding. The average of these metrics across all modalities is shown in Figure 5. Importantly, as modal sparsity is increased, the number of unimodal samples decreases proportionally, while some fusion samples are dropped from the set of embeddings when all unimodal samples have been dropped by the procedure of introducing modal sparsity. While this prevents a direct comparison of metrics between datasets preprocessed with different modal sparsity, it is still useful as a comparison between MCA and MMA models.

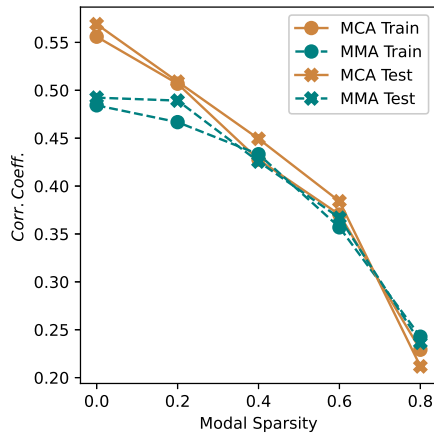
The average median rank of unimodal test split embeddings is improved in MCA over MMA. In the larger CMU-MOSEI dataset, the difference is greatest at high modal sparsity. In the smaller TCGA dataset, it is greatest at low modal sparsity. This may be due to better uniformity and worse alignment in MCA. At the highest sparsity of 0.8,

there is an average number of modalities per sample of $\bar{\mu} > 1$ and the average median rank drops significantly. This may be attributed to a fewer number of unimodal and fusion embeddings.

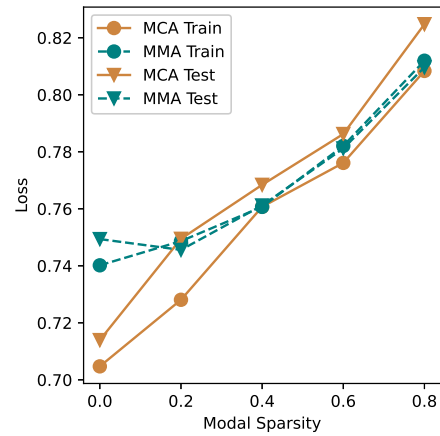
The recall metrics (R_1 , R_5 , and R_{10}) show the capability of the unimodal embedding spaces to be used to identify matching fusion embeddings. MCA has improved recall metrics over MMA for most modal sparsities examined in both datasets. Similar to the average median rank metrics, the smaller TCGA dataset shows the best recall metric improvement of MCA at low modal sparsity. For the larger CMU-MOSEI dataset, the improvement is smaller and may be within the range of model variation due to hyperparameter selection and choice of evaluation epoch, yet MCA has higher recall metrics than MMA for most modal sparsities studied. The results show the utility of using MCA as a method of retrieving embedding containing information from multiple modalities, even when only a single modality is available at inference time and training examples contain only sparsely aligned modalities.

6.1 Task Performance

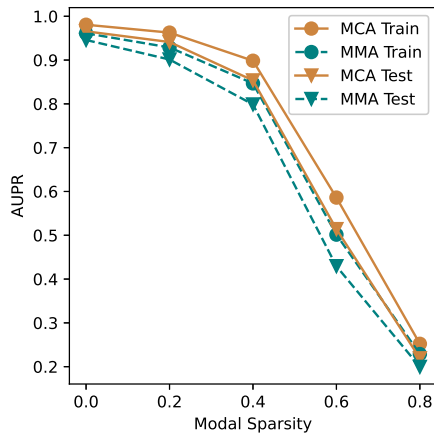
The analysis of the generated embeddings on downstream tasks is a crucial component of validating model performance. In this section the linear probing performance of embeddings as a function of modal sparsity is demonstrated. A linear layer is trained using embeddings produced from the dataset training split using either L1 loss for regression or cross entropy loss for classification. The metrics displayed in Figure 6 are calculated using the trained linear model



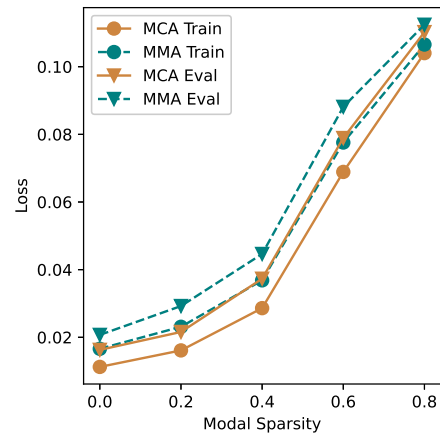
(a) Average AUPR value for multi-class classification of TCGA tumor type.(\uparrow)



(b) Correlation between true and predicted values for CMU-MOSEI sentiment regression task.(\downarrow)



(c) Average AUPR value for multi-class classification of TCGA tumor type.(\uparrow)



(d) Correlation between true and predicted values for CMU-MOSEI sentiment regression task.(\downarrow)

Figure 6: Comparison of performance of MCA and MMA on linear probing tasks of generated embedding spaces for validation split datasets.

to run inference on test dataset splits which have not been used to train the embeddings or the linear probe. Importantly, no pretrained model weights are relaxed in this evaluation. All tasks are thus a direct linear probing of the generated embedding spaces for the test dataset splits. In general MCA provides improved results over MMA for both datasets.

The task performed for the TCGA dataset is a multiclass problem with 32 classes. These correspond to the type of cancer present in the specimen from which a sample was generated. The class-averaged area under the precision-recall curve (AUPR) is presented in Figure 6. Both MCA and MMA perform well, while MCA shows a slightly increasing level of improvement over MMA as modal sparsity is increased to 0.4.

The CMU-MOSEI sentiment analysis task is a regression to a single value. This value ranges between 0 and 1, corresponding to negative and positive sentiment. In the initial study describing the CMU-MOSEI dataset, a correlation coefficient of 0.54 is achieved using an LSTM-based modal fusion architecture. [31] While better correlation coefficients for this dataset have been demonstrated more recently, this result is taken as the baseline for evaluation. MCA is able to meet this baseline result with only linear regression of the produced embeddings when no modal sparsity is present. As modal sparsity is increased the correlation coefficient is reduced, and MCA and MMA results become similar with a minor increase in MCA vs. MMA.

7 Conclusion

Masked multimodal transformer architectures can learn embedding spaces robust to missing modalities. Multichannel attention was presented as an extension of the masked multimodal transformer model and incorporates modal-incomplete channels in the multihead attention mechanism. Using two well-known datasets, each with four modalities, both MMA and MCA are shown to learn high quality embedding spaces up to a modal sparsity of 0.4, corresponding to 1-2 modalities most frequently missing per sample for the datasets studied here. We find that MCA generally improves the quality of embedding spaces, recall metrics, and subsequent performance on downstream tasks.

Future directions for research could extend the architecture presented here to autoencoding or joint embedding predictive architectures for multimodal transformers, explore multimodal scaling laws with modal sparsity, and explore foundational model scale datasets for multimodal representation learning with sparsely aligned datasets.

8 Acknowledgments

The author thanks Clayton Rabideau, Gabrielle Griffin, Callum Birch-Sykes and Archis Joglekar for helpful conversations in the course of this study. The results shown here are in whole or part based upon data generated by the TCGA Research Network: <https://www.cancer.gov/tcga>.

References

- [1] Peng Xu, Xiatian Zhu, and David A Clifton. Multimodal learning with transformers: A survey. *IEEE Transactions on Pattern Analysis and Machine Intelligence*, 2023.
- [2] Xue Han, Yi-Tong Wang, Jun-Lan Feng, Chao Deng, Zhan-Heng Chen, Yu-An Huang, Hui Su, Lun Hu, and Peng-Wei Hu. A survey of transformer-based multimodal pre-trained modals. *Neurocomputing*, 515:89–106, 2023.
- [3] Paul Pu Liang, Amir Zadeh, and Louis-Philippe Morency. Foundations and recent trends in multimodal machine learning: Principles, challenges, and open questions. *arXiv preprint arXiv:2209.03430*, 2022.
- [4] Allen W Lynch, Christina V Theodoris, Henry W Long, Myles Brown, X Shirley Liu, and Clifford A Meyer. Mira: joint regulatory modeling of multimodal expression and chromatin accessibility in single cells. *Nature Methods*, 19(9):1097–1108, 2022.
- [5] Kari A Noriy, Xiaosong Yang, Marcin Budka, and Jian Jun Zhang. Clara: Multilingual contrastive learning for audio representation acquisition. *arXiv preprint arXiv:2310.11830*, 2023.
- [6] Hassan Akbari, Liangzhe Yuan, Rui Qian, Wei-Hong Chuang, Shih-Fu Chang, Yin Cui, and Boqing Gong. Vatt: Transformers for multimodal self-supervised learning from raw video, audio and text. *Advances in Neural Information Processing Systems*, 34:24206–24221, 2021.
- [7] Amanpreet Singh, Ronghang Hu, Vedanuj Goswami, Guillaume Couairon, Wojciech Galuba, Marcus Rohrbach, and Douwe Kiela. Flava: A foundational language and vision alignment model. In *Proceedings of the IEEE/CVF Conference on Computer Vision and Pattern Recognition*, pages 15638–15650, 2022.

- [8] Alec Radford, Jong Wook Kim, Chris Hallacy, Aditya Ramesh, Gabriel Goh, Sandhini Agarwal, Girish Sastry, Amanda Askell, Pamela Mishkin, Jack Clark, et al. Learning transferable visual models from natural language supervision. In *International conference on machine learning*, pages 8748–8763. PMLR, 2021.
- [9] Jean-Baptiste Alayrac, Adria Recasens, Rosalia Schneider, Relja Arandjelović, Jason Ramapuram, Jeffrey De Fauw, Lucas Smaira, Sander Dieleman, and Andrew Zisserman. Self-supervised multimodal versatile networks. *Advances in Neural Information Processing Systems*, 33:25–37, 2020.
- [10] Po-Yao Huang, Mandela Patrick, Junjie Hu, Graham Neubig, Florian Metze, and Alexander Hauptmann. Multilingual multimodal pre-training for zero-shot cross-lingual transfer of vision-language models. *arXiv preprint arXiv:2103.08849*, 2021.
- [11] Nanyi Fei, Zhiwu Lu, Yizhao Gao, Guoxing Yang, Yuqi Huo, Jingyuan Wen, Haoyu Lu, Ruihua Song, Xin Gao, Tao Xiang, et al. Towards artificial general intelligence via a multimodal foundation model. *Nature Communications*, 13(1):3094, 2022.
- [12] Po-Yao Huang, Vasu Sharma, Hu Xu, Chaitanya Ryali, Yanghao Li, Shang-Wen Li, Gargi Ghosh, Jitendra Malik, Christoph Feichtenhofer, et al. Mavil: Masked audio-video learners. *Advances in Neural Information Processing Systems*, 36, 2024.
- [13] Paul Hager, Martin J Menten, and Daniel Rueckert. Best of both worlds: Multimodal contrastive learning with tabular and imaging data. In *Proceedings of the IEEE/CVF Conference on Computer Vision and Pattern Recognition*, pages 23924–23935, 2023.
- [14] Jean-Baptiste Alayrac, Jeff Donahue, Pauline Luc, Antoine Miech, Iain Barr, Yana Hasson, Karel Lenc, Arthur Mensch, Katherine Millican, Malcolm Reynolds, et al. Flamingo: a visual language model for few-shot learning. *Advances in Neural Information Processing Systems*, 35:23716–23736, 2022.
- [15] Wasifur Rahman, Md Kamrul Hasan, Sangwu Lee, Amir Zadeh, Chengfeng Mao, Louis-Philippe Morency, and Ehsan Hoque. Integrating multimodal information in large pretrained transformers. In *Proceedings of the conference. Association for Computational Linguistics. Meeting*, volume 2020, page 2359. NIH Public Access, 2020.
- [16] David Mizrahi, Roman Bachmann, Oguzhan Kar, Teresa Yeo, Mingfei Gao, Afshin Dehghan, and Amir Zamir. 4m: Massively multimodal masked modeling. *Advances in Neural Information Processing Systems*, 36, 2024.
- [17] Nina Shvetsova, Brian Chen, Andrew Rouditchenko, Samuel Thomas, Brian Kingsbury, Rogerio S Feris, David Harwath, James Glass, and Hilde Kuehne. Everything at once-multi-modal fusion transformer for video retrieval. In *Proceedings of the IEEE/CVF conference on computer vision and pattern recognition*, pages 20020–20029, 2022.
- [18] Adrià Recasens, Jason Lin, João Carreira, Drew Jaegle, Luyu Wang, Jean-baptiste Alayrac, Pauline Luc, Antoine Miech, Lucas Smaira, Ross Hemsley, et al. Zorro: the masked multimodal transformer. *arXiv preprint arXiv:2301.09595*, 2023.
- [19] Siddharth Srivastava and Gaurav Sharma. Omnivec: Learning robust representations with cross modal sharing. In *Proceedings of the IEEE/CVF Winter Conference on Applications of Computer Vision*, pages 1236–1248, 2024.
- [20] Junjie Shi, Li Yu, Qimin Cheng, Xin Yang, Kwang-Ting Cheng, and Zengqiang Yan. M2ftrans: Modality-masked fusion transformer for incomplete multi-modality brain tumor segmentation. *IEEE Journal of Biomedical and Health Informatics*, 2023.
- [21] Yao Zhang, Nanjun He, Jiawei Yang, Yuexiang Li, Dong Wei, Yawen Huang, Yang Zhang, Zhiqiang He, and Yefeng Zheng. mmformer: Multimodal medical transformer for incomplete multimodal learning of brain tumor segmentation. In *International Conference on Medical Image Computing and Computer-Assisted Intervention*, pages 107–117. Springer, 2022.
- [22] Karren Dai Yang, Anastasiya Belyaeva, Saradha Venkatachalapathy, Karthik Damodaran, Abigail Katcoff, Adityanarayanan Radhakrishnan, GV Shivashankar, and Caroline Uhler. Multi-domain translation between single-cell imaging and sequencing data using autoencoders. *Nature communications*, 12(1):31, 2021.
- [23] Yunhua Zhang, Hazel Doughty, and Cees GM Snoek. Learning unseen modality interaction. *arXiv preprint arXiv:2306.12795*, 2023.
- [24] Tongzhou Wang and Phillip Isola. Understanding contrastive representation learning through alignment and uniformity on the hypersphere. In *International Conference on Machine Learning*, pages 9929–9939. PMLR, 2020.
- [25] Manuel Tran, Amal Lahiani, Yashin Dicente Cid, Fabian J Theis, Tingying Peng, and Eldad Klaiman. Training transitive and commutative multimodal transformers with loretta. *arXiv preprint arXiv:2305.14243*, 2023.

- [26] Shicai Wei, Yang Luo, and Chunbo Luo. One-stage modality distillation for incomplete multimodal learning. *arXiv preprint arXiv:2309.08204*, 2023.
- [27] Ryumei Nakada, Halil Ibrahim Gulluk, Zhun Deng, Wenlong Ji, James Zou, and Linjun Zhang. Understanding multimodal contrastive learning and incorporating unpaired data. In *International Conference on Artificial Intelligence and Statistics*, pages 4348–4380. PMLR, 2023.
- [28] Emma L Tonkin, Michael Holmes, Hao Song, Niall Twomey, Tom Diethe, Meelis Kull, Miquel Perello Nieto, Massimo Camplani, Sion Hannuna, Xenofon Fafoutis, et al. A multi-sensor dataset with annotated activities of daily living recorded in a residential setting. *Scientific Data*, 10(1):162, 2023.
- [29] Can Cui, Haichun Yang, Yaohong Wang, Shilin Zhao, Zuhayr Asad, Lori A Coburn, Keith T Wilson, Bennett Landman, and Yuankai Huo. Deep multi-modal fusion of image and non-image data in disease diagnosis and prognosis: a review. *Progress in Biomedical Engineering*, 2023.
- [30] Victor Weixin Liang, Yuhui Zhang, Yongchan Kwon, Serena Yeung, and James Y Zou. Mind the gap: Understanding the modality gap in multi-modal contrastive representation learning. *Advances in Neural Information Processing Systems*, 35:17612–17625, 2022.
- [31] Amir Zadeh, Paul Pu Liang, Soujanya Poria, Prateek Vij, Erik Cambria, and Louis-Philippe Morency. Multi-attention recurrent network for human communication comprehension. In *Thirty-Second AAAI Conference on Artificial Intelligence*, 2018.
- [32] John N Weinstein, Eric A Collisson, Gordon B Mills, Kenna R Shaw, Brad A Ozenberger, Kyle Ellrott, Ilya Shmulevich, Chris Sander, and Joshua M Stuart. The cancer genome atlas pan-cancer analysis project. *Nature genetics*, 45(10):1113–1120, 2013.
- [33] Adam Paszke, Sam Gross, Francisco Massa, Adam Lerer, James Bradbury, Gregory Chanan, Trevor Killeen, Zeming Lin, Natalia Gimelshein, Luca Antiga, et al. Pytorch: An imperative style, high-performance deep learning library. *Advances in neural information processing systems*, 32, 2019.

9 Additional Figures

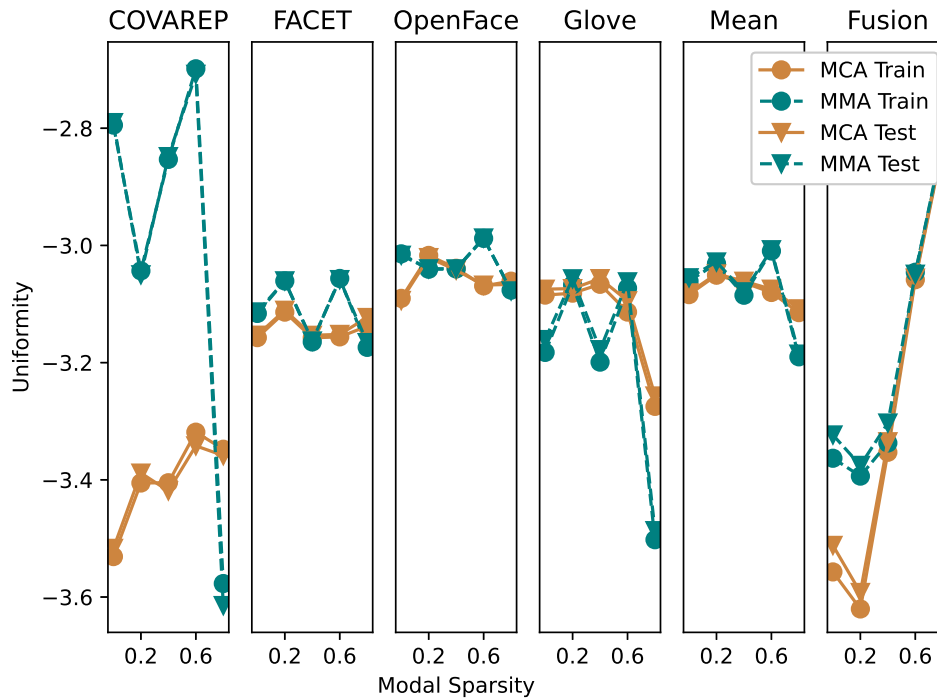


Figure 9.7: Uniformity of embeddings for CMU-MOSEI dataset.

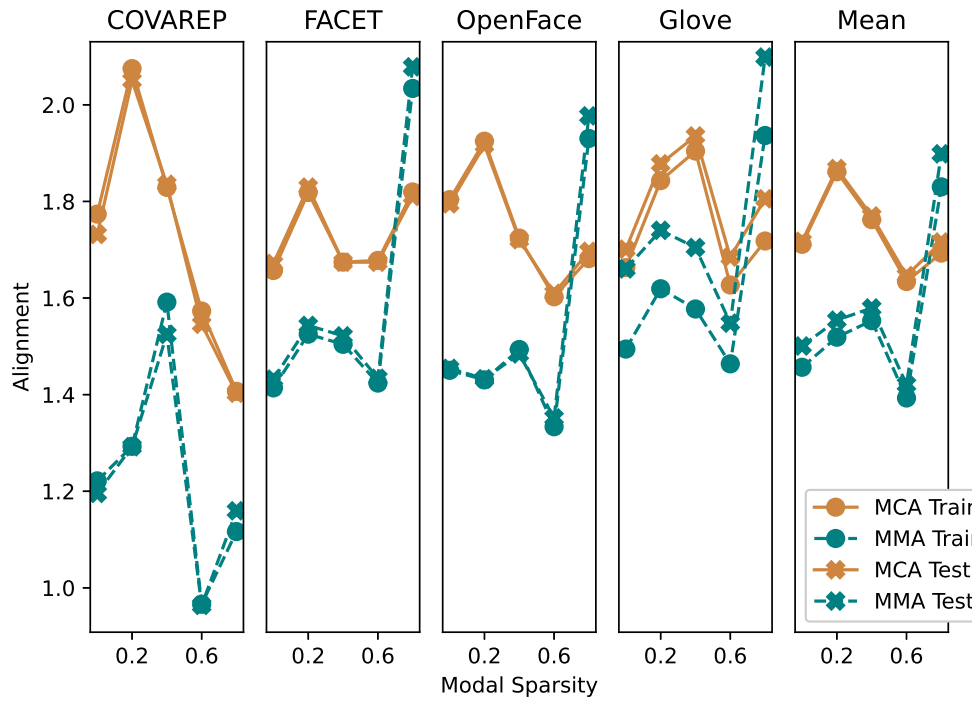


Figure 9.8: Alignment of embeddings for CMU-MOSEI dataset.

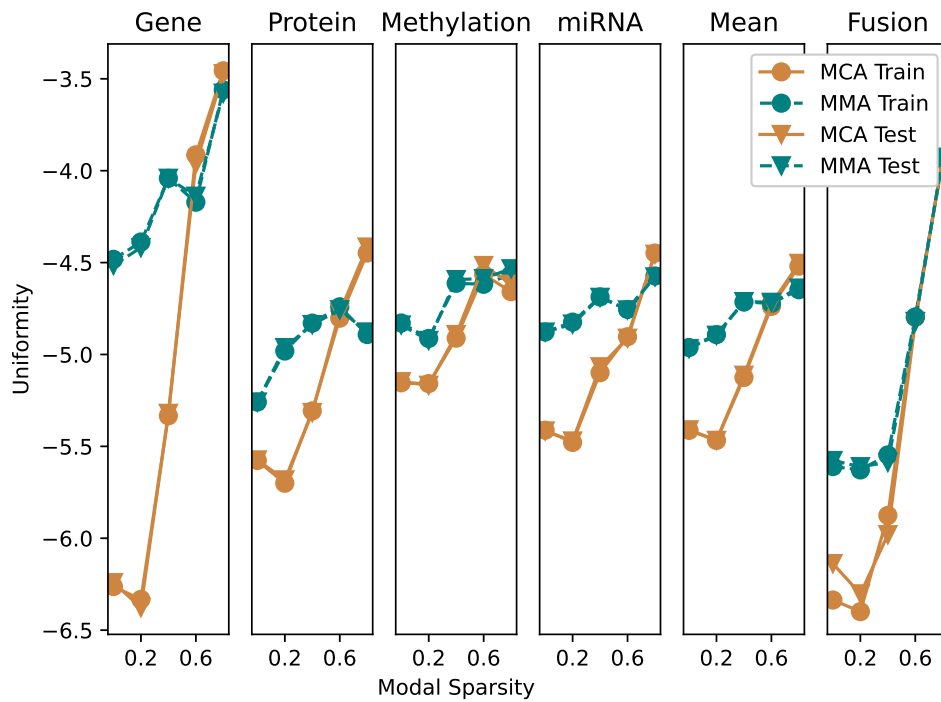


Figure 9.9: Uniformity of embeddings for TCGA dataset.

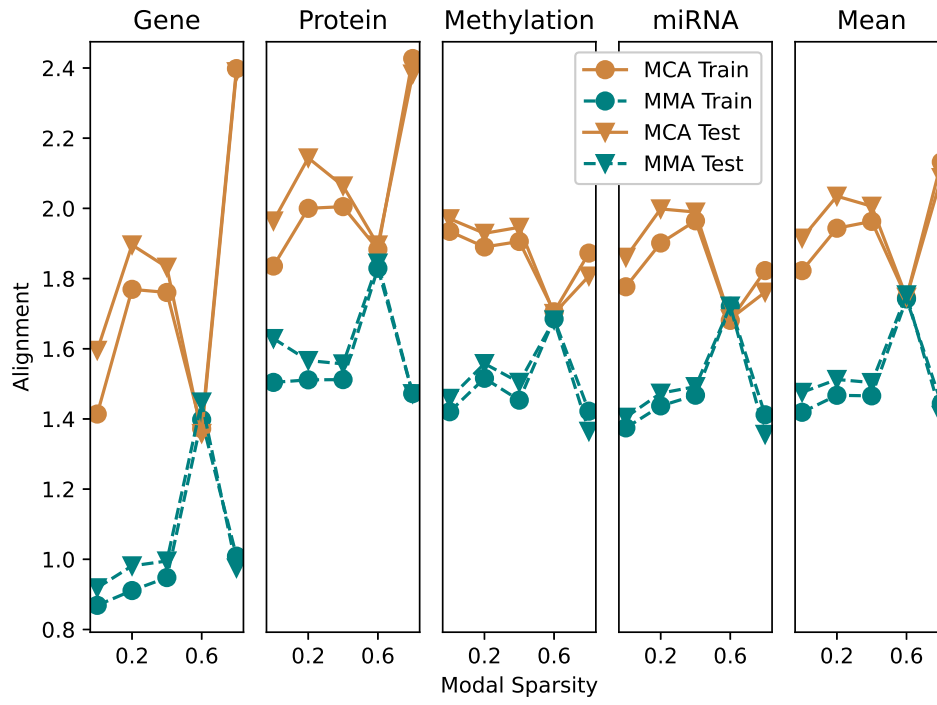


Figure 9.10: Alignment of embeddings for TCGA dataset.